JOURNAL OF DEGRADED AND MINING LANDS MANAGEMENT
Volume 12, Number 1 (October 2024):6849-6864, doi:10.15243/jdmlm.2024.121.6849
ISSN: 2339-076X (p); 2502-2458 (e), www.jdmlm.ub.ac.id

Research Article

Water holding capacity, aggregation, respiration, and chemical character of acid soil amended rice straw biochar enriched with different volumes of liquid extract (sap) of *Kappapychus alvarezii*

Fransiscus Suramas Rembon[1*], Laode Muhammad Harjoni Kilowasid[2], La Ode Afa[2], Tresjia Corina Rakian[2], Imelia Parapa[2], Muhammad Alfi Nanda Laksana[2], Laode Sabaruddin[2], Azhar Ansi[2], La Ode Ahmad Nur Ramadhan[3], Dahlan[4], Zulfikar[1]

[1] Department of Soil Science, Halu Oleo University, Kendari, 93232, Indonesia
[2] Department of Agrotechnology, Halu Oleo University, Kendari, 93232, Indonesia
[3] Department of Chemistry, Halu Oleo University, Kendari, 93232, Indonesia
[4] Department of Chemistry Education, Halu Oleo University, Kendari, 93232, Indonesia

[*]corresponding author: fransrembon@yahoo.com

Article history:
Received 9 July 2024
Revised 27 August 2024
Accepted 6 September 2024

Keywords:
aluminum
carbon
cation
soil management
soil quality

Abstract

The quality of acidic soil is determined by organic C content produced from rice straw biochar in agriculture. In this context, liquid extract from *Kappapychus alvarezii* (K-sap) is used as a biochar enrichment agent. Therefore, this research aimed to (i) analyze the character of K-sap enriched rice straw biochar with different volumes, as well as (ii) evaluate the impact on soil water holding capacity, size class distribution, aggregate stability index, respiration rate, and acidic soil chemical characters. The treatment tested was the volume of K-sap kg^{-1} biochar, namely (i) without biochar, (ii) 0 mL, (iii) 500 mL, (iv) 1,000 mL, and (v) 1,500 mL. Each treatment was repeated three times and placed according to a randomized block design procedure. The area covered by K-sap, pore size, and amorphous degree increased while the pore volume of the biochar surface decreased. The addition of 1,000 mL of K-sap kg^{-1} biochar released a new peak number associated with the aliphatic and aromatic groups. The K-sap enriched biochar increased the proportion of soil aggregate size of 1-2 mm, water holding capacity, carbon storage, pH, total N, available P and K, exchangeable base cations as well as base saturation. Meanwhile, the concentration of Al^{3+} and H^{+} were decreased in the acidic soil solution. The results showed that the performance of rice straw biochar, K-sap volumes, soil chemical quality, water holding capacity, and ability to store carbon of the acidic soil was improved by adding K-sap volume.

To cite this article: Rembon, F.S., Kilowasid, L.M.H., Afa, L.O., Rakian, T.C., Parapa, I., Laksana, M.A.N., Sabaruddin, L., Ansi, A., Ramadhan, L.O.A.N., Dahlan, and Zulfikar. 2024. Water holding capacity, aggregation, respiration, and chemical character of acid soil amended rice straw biochar enriched with different volumes of liquid extract (sap) of *Kappapychus alvarezii*. Journal of Degraded and Mining Lands Management 12(1):6849-6864, doi:10.15243/jdmlm.2024.121.6949.

Introduction

The addition of organic matter is recommended by sustainable management of degraded agricultural land to improve the quality and fertility of acidic clay soils in tropical environments (Stocking, 2003; Purwanto and Alam, 2020; Momesso et al., 2022). The low organic matter content in acidic clay has implications for cation exchange capacity and soil capacity to hold low water. The content of Al^{3+} and H^{+} ions as well as the percentage of microaggregates, can be increased (Mokolobate and Haynes, 2002; Soliman and

Mansour, 2024). The adsorption capacity of Al^{3+} ions can be decreased by soils with low organic matter due to the high solubility, contributing to the increase in H^+ ions and the acidic nature of the soil (Baquy et al., 2018; Jiang et al., 2018). The capacity to hold water, ion exchange capacity, soil aggregation, and biological activities, including respiration and mineralization of carbon, are also affected by a carbon functional group (Audette et al., 2021; Cheng et al., 2021; Ramírez et al., 2023). In this context, the surface inhibits the production and solubility of Al^{3+} ions through the formation of $Al(OH)_3$ (Jones et al., 1996; Li et al., 2023; Shan and Riaz, 2023).

Agricultural solid waste serves as a source of raw materials in producing organic fertilizers in the form of compost, vermicompost, and biochar to improve the quality and fertility of acidic soils (Chew et al., 2019; Enaime and Lübken, 2021). In Indonesia, rice straw waste is abundant, and the biochemical composition consists of cellulose, hemicellulose, lignin, and silica ranging from 37.60-46.55%, 22.35-28.25%, 5.60-11.60%, and 9.05-13.70%, respectively (Malik et al., 2023). The biomass component contains an OH functional group of alcohol as well as aldehyde, ketones, ether, and aromatic rings (Liu et al., 2022). In addition, the application increases the organic C content and the aggregation of clay (Halder et al., 2023). The use of agricultural solid waste as feedstock of biochar production for soil conditioner materials and organic biochar-based fertilizers to improve the quality and fertility of agricultural soil continues to be developed (Jamilatun et al., 2022; Mutolib et al., 2023). The application of rice straw biochar for agricultural productivity is directed at increasing soil pH, capacity to store and retain water, organic C, storage in soil, nutrients available, aggregate formation, and reduction of Al solubility (Islam et al., 2021; Bolan et al., 2023). pH, organic C, cation exchange capacity, base saturation, available P, and exchangeable base cations in acidic soils can be improved using biochar (Yuan et al., 2022; Shi et al., 2023; Zhang et al., 2023). The physicochemical characteristics of biochar are related to the ability to store and retain water, as well as the chemical fertility component of acidic soil. Moreover, surface pores play an important role in retaining water, OH, and COOH groups (Kilowasid et al., 2023). The size distribution of aggregates can be changed through the application without affecting the stability and soil respiration in tropical environments (Zhou et al., 2017; Ghorbani et al., 2019). Soil respiration is the main pathway of CO_2 efflux from agricultural land released into the atmosphere (Luan et al., 2020; Basheer et al., 2024). Therefore, a strategy is needed to adapt the technology of using organic matter in agronomic practices to improve soil quality and agricultural land (Don et al., 2024; Grados et al., 2024; Petersson et al., 2024).

Enrichment methods using inorganic and liquid organic fertilizers improve the performance of biochar to reduce greenhouse gas emissions from agricultural land (Mohammadi et al., 2016; Ndoung et al., 2021). This can also change the morphological surface and chemical character of biochar (Nardis et al., 2021), and *K. alvarezii* can produce organic fertilizer (Bajpai et al., 2024; van Tol de Castro et al., 2024). Several coasts of Indonesia produce seaweed of species *K. alvarezzi* (Simatupang et al., 2021). A liquid extract from *K. alvarezzi* (K-sap) cultivated in the coastal area contains compounds associated with biostimulant substances, including kinetin and indole acetic acid (Fadilah et al., 2016), as well as essential macro and micronutrients (Rakian et al., 2023). Currently, the use of K-sap to enrich biochar continues to be developed. Kilowasid et al. (2023) stated that the addition of different concentrations of K-sap changes the morphological surface, chemical composition, characteristics of the absorption band, and peak wave number of rice straw biochar. At a dose of 10% soil weight, the application of enriched biochar increased pH, organic C, total N, C: N ratio, electrical conductivity of 1.07 dS cm^{-1}, available P, exchangeable Ca, Mg, and K, as well as the content of Si in acidic soil. The influence of K-sap volume in the development of biochar enriched with seaweed liquid extract should be considered as an organic fertilizer for agricultural acidic soil conditioning. Therefore, this research aimed to (i) analyze the characteristics of K-sap enriched rice straw biochar from different volumes, and (ii) evaluate the impact on soil water holding capacity, size class distribution and aggregate stability index, respiration rate, as well as soil chemical characters.

Materials and Methods

Site and experimental design

This experiment was carried out at the Agronomy Laboratory, Faculty of Agriculture, Halu Oleo University, from May to October 2022. The ratio of the volume of K-sap solution applied based on the weight of biochar (v/b) consisted of 4 : (i) 0 mL (RSB0), (ii) 500 mL (RSB500), (iii) 1,000 mL (RSB1000), and (iv) 1,500 mL of K-sap (RSB1500). A kilogram of rice straw biochar (RSB) was added to each volume of K-sap. Therefore, the five treatments of the soil included (i) without biochar (B0), (ii) addition of 0 mL (RSB0), (iii) 500 mL (RSB500), (iv) 1,000 mL (RSB1000), and (v) 1,500 mL of K-sap enriched biochar (RSB1500). The treatment was repeated three times and placed according to the randomized block design pattern.

Preparation of biochar and K. alvarezii sap

Rice straw biochar was produced through incomplete combustion in a drum for four hours at a temperature of 320 °C (Kilowasid et al., 2023). The product was converted from the straw sprinkled with water to prevent further combustion. The air-dry biochar with a moisture content of 18% was crushed using a flour machine equipped with a <3 mm filter, and stored in a

plastic container. Meanwhile, 36-day-old *Kappapychus alvarezii* seaweed was taken from the cultivation site in the coastal waters of Tanjung Tiram, Kendari City. Sand, mud deposits, and other materials attached to the talus were removed using seawater. Subsequently, the talus was chopped manually and mashed using a kitchen blender without adding water until porridge was formed. The talus slurry was filtered before accommodating the extract (K-sap) in a plastic container and stored in a room with a temperature of 4-5 ºC.

Biochar enriched with K-sap

The dose of biochar used was based on the percentage of the weight before K-sap enrichment to soil weight. In addition, the tested dose is 5% of the weight of the soil (Kilowasid et al., 2023). K-sap was diluted using tap water to a concentration level of 10%, and each volume was poured into a plastic container, mixed evenly, and stored in a cetic bag. A total of 50 g of each biochar enriched with different volume treatments was taken to scan Electron Microscope–Energy Dispersive Spectroscopy (SEM-EDS) at the Mechanical Engineering Laboratory of the Surabaya Institute of Technology. Surface area and pore analysis, infrared spectrum, and diffraction were carried out using Brunauer-Emmett-Teller (BET) Quantachrome Nova 4200e, Fourier-Transform Infrared Spectrometer (FTIR), and X-Ray Diffraction (XRD) at the National Research and Innovation Agency (BRIN) Laboratory, respectively.

Application of biochar-enriched with K-sap into soil

The acidic soil of an Ultisol was taken to a depth of 10 cm from an upland rice field in Amoito Jaya Village, District Wolasi, South Konawe Regency. The characteristics contain 11% sand, 61% silt, 28% clay fraction, 4.9 soil pH, 0.11% total N content, 29 mg100 g^{-1} P_2O_5 total P and 12 mg 100 g^{-1} K_2O total K. Meanwhile, air-dried soil samples were sifted with a size of <5 mm/opening and stored until use. A total of 5 kg of acidic soil that passed through the sieve was added with 250 g of biochar-enriched K-sap (the dose used was 5% of the weight of biochar before being enriched with K-sap from the weight of the soil) in a plastic container, then mixed homogeneously. The mixture of soil and biochar-enriched K-sap was put into different experimental pots, saturated with water, and incubated under room conditions in the greenhouse. After 14 days of incubation, 500 g of soil was taken from each pot for measurement of pH using a pH meter in 1:5 of soil-water suspension, determination of organic C using the Walkley and Black method, total N using Kjeldahl, C/N ratio, cation exchangeable capacity (CEC) with NH_4-acetate 1N at pH 7, and Al^{3+} and H^+ using KCl 1N. The analysis of these soil chemical parameters used the soil chemical test protocol at the Soil Testing Laboratory of Soil Research Institute in Bogor. The remaining soil was used for the purpose of determining water-holding capacity and retention, soil aggregate, and soil respiration.

Determination of soil water-holding capacity and retention

A total of 200 g of soil was mixed with biochar enriched with different volumes of K-sap. The solution was put into different PVC tubes whose bottoms were covered with two layers of 200 mesh nylon fabric, weighed, and recorded as W value. Subsequently, the soil is poured with tap water slowly until the water flows outward from the bottom of the tube in room conditions. In the absence of dripping, the mixture was weighed and recorded as a W_1 value. For soil treated with rice straw biochar and enriched with a different volume of K-sap using the following formula, W_0 value, and W_1 are the values of the water holding capacity (Lü et al., 2016).

$$W(\%) = \frac{W_1 - W_0}{200} \text{ x } 100$$

W value was obtained by analyzing the water-holding capacity, and the biochar was enriched with different volumes of K-sap every day for 39 days. The following equation was used to obtain the water retention value (W_r) (Lü et al., 2016) W_r (%) = $\frac{W_1 - W_0}{200}$ x 100

Determination of size distribution class and stability index for soil aggregate

The distribution of aggregate size classes was determined by dry and wet sieving methods (Obalum et al., 2019). A total of four filters measuring 4 mm, 2 mm, 1 mm, and 0.25 mm/opening are arranged from top to bottom in a row from the largest opening to the smallest. There is a micro aggregate reservoir passing through the filter at the bottom of the smallest opening. In the uppermost filter, 40 g of soil aggregate is placed and swung up and down for 5 minutes with an oscillation of 35 minutes. In this context, the soil aggregate held on each filter is drained at 105 ºC for 16.5 hours. The average dry weight was weighed and calculated using the formula $MWD_d = (X\sum_{i=1}^{n} iWi)$, where MWDd states the average weight of a dry sieve of an aggregate class, Xi expresses the diameter of the fraction of size class i (mm), W_i is the proportion of the total weight in a fraction of a given size (g g^{-1}), and n is the aggregate size held in each sieve and collecting tub under the nest.

From the sifting procedure, 40 g of soil aggregate was placed in the uppermost filter. Subsequently, the filter pile was swung up and down until the water surface was touched with an amplitude of 4 cm and an oscillation of 35 per minute. The sieve containing soil aggregate was immersed in a puddle of water for five minutes, followed by oscillations for one minute. The waterproof aggregate (WSA) retained in each filter was transferred into a different aluminum dish and dried using an oven. Finally, the average dry weight of the sieve was calculated with the formula $MWD_w = (X\sum_{i=1}^{n} iWi)$, where MWD_w expresses the diameter of

the aggregate weight of the wet sieve, X_i is the diameter of the size (mm), W_i is the proportion of the aggregate in a fraction of a given size (g g^{-1}), and n is the total number of fractions of aggregate size held in each sieve and collector tub. The stability of soil aggregates was determined using the wet sifting method (wet sieving). After wet sifting, the soil held on each sieve was transferred into an aluminum cup and dried at 105 °C for 16.5 hours using an oven. Meanwhile, the WSA was dispersed with NaOH 0.1 N before washing the slurry through a 0.25 mm sieve to obtain a sand mass of >0.25 mm (SW). The stability of the soil aggregate was defined as percent WSA, and the index value (ISA) was calculated using the formula of Obalum et al. (2019).

$$\text{ISA} = \frac{\text{WSA} - \text{SW}}{\text{initial aggregate weight} - \text{SW}}\ x\ 100\%$$

Determination of CO_2-flux of soil

Soil respiration is determined through the acid-base titration method (FAO, 2023). A total of 100 g of soil that was treated with rice straw biochar at different volumes of K-sap was put into a jar container. In this context, the two PVC bottles contained 10 mL of KOH 0.1 N and distilled water. The jars were tightly closed and incubated in a dark room at room temperature. After 14, 28, 42, 56, and 70 days, KOH was titrated by adding two drops of phenolphthalein marker to form a pink color. The solution was titrated with HCl until the KOH solution turned clear, and the volume of HCl released from the burette was recorded. The distilled water solution was added to two drops of methyl orange to form a yellow color and titrated with HCl. The process resulted in a pink color, and the amount of CO_2 released was calculated using the following formula.

$$\text{r} = \frac{(\text{a} - \text{b})\ \text{x N x}\ 120}{\text{t}}$$

where: a is mL HCl for the sample, b is mL HCl for the control, N is the normality of HCl, t is the number of incubation days, and r is C–CO_2 produced per gram of soil per day.

Statistical analysis

The amount of CO_2 released and soil chemical character parameters were examined using analysis of variance (ANOVA) to determine the effect of the volume ratio of K-sap on biochar weight of soil moisture content, water storage capacity, distribution of size classes, and aggregation stability index. Another test was carried out to distinguish the difference between treatments using the Least Significant Difference Test (LSD) at $p<0.05$ level when the ANOVA showed a significant effect. Meanwhile, the rate of CO_2 release from soil was estimated using a regression model.

Results

Image SEM-EDS of the enriched-biochar surface

Image SEM in Figures 1a, 1b, 1c, and 1d show the surface of the dried biochar without gel covering. Biochar without K-sap (RSB0) has a hollow surface (Figure 1a), and the increase in volume decreases the cavity, as shown in Figures 1b, 1c, and 1d.

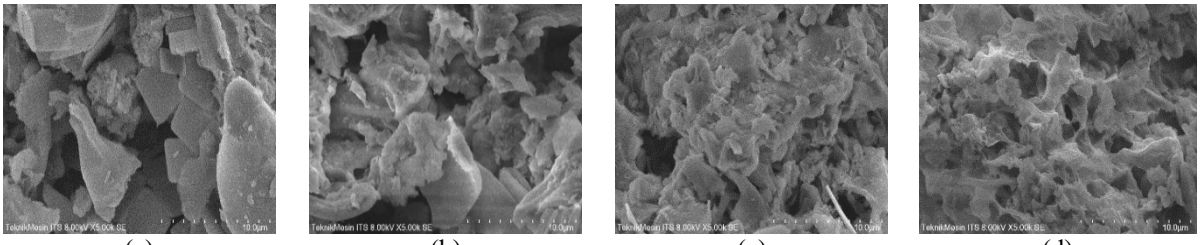

(a) (b) (c) (d)

Figure 1. SEM Image of surface morphology of rice straw biochar enriched in different volumes of K-sap. (a) RSB0, (b) RSB500, (c) RSB1000, and (d) RSB1500.

EDS analysis (Table 1) showed that the proportions of elements C, Na, Fe, Al, Mn, and Mo were detected most in 500 mL of K-sap enriched biochar (RSB500). The elements O, N, and Mg were most abundant in 1,500 mL of enriched biochar of K-sap. In unenriched biochar (RSB0), the most detected elements were P and Se. The elements K, Ca, Si, and Zn were detected in biochar enriched with 1,000 mL of K-sap (RSB1000).

BET analysis of the enriched-biochar

The results of BET analysis (Table 2) showed that the surface area (m^2 g^{-1}) of rice straw biochar after enrichment decreased, respectively with the increase of K-sap volume, in order from narrowest to widest, RSB0 (42.93 m^2 g^{-1}) > RSB500 (34.53 m^2 g^{-1}), > RSB1000 (27.31 m^2 g^{-1}), > RSB1500 (26.62 m^2 g^{-1}). Pore volume increased from RSB0 (0.106 cc g^{-1}) to RSB500 (0.112 cc g^{-1}), then decreased with increasing K-sap volume, respectively RSB1000 (0.092 cc g^{-1}) > RSB1500 (0.087 cc g^{-1}).

The average pore size of biochar increased with increasing volume of K-sap, respectively in order from smallest to largest pore radius were RSB0 (99.08 Å) > RSB500 (125.82 Å) > RSB1000 (134.76 Å) > RSB1500 (135.42 Å).

Table 1. Elemental composition in rice straw biochar enriched with different volumes of K-sap.

Elements	Unit (w/w)	Rice straw biochar enriched with different volumes of K-sap			
		RSB0	RSB500	RSB1000	RSB1500
C	%	7.63	16.87	5.81	8.99
O	%	46.15	33.56	40.40	46.87
N	%	4.06	3.45	3.13	4.08
P	%	0.97	0.82	0.64	0.81
K	%	4.66	7.46	7.82	4.40
Na	%	nd	0.55	0.35	0.39
Ca	%	2.65	3.04	6.94	2.52
Mg	%	0.64	0.92	0.72	1.04
Si	%	30.32	27.07	30.45	26.41
Fe	%	nd	0.84	nd	0.78
Al	%	nd	1.50	0.81	1.46
Mn	%	nd	1.07	0.59	nd
Mo	%	1.45	1.87	0.90	1.46
Zn	%	1.01	0.97	1.29	0.80
Se	%	0.45	nd	0.17	nd

Notes: nd = not detected. RSB0 = 0 mL of K-sap enriched biochar, RSB500 = 500 mL of K-sap enriched biochar, RSB1000 = 1,000 mL of K-sap enriched biochar, and RSB1500 = 1,500 mL of K-sap enriched biochar.

Table 2. The surface area, pore volume, and average pore radius of rice straw biochar between the difference in K-sap volume to biochar weight.

Treatments	SA (m^2 g^{-1})	PV (cc g^{-1})	AP (Å)
RSB0	42.93	0.106	99.08
RSB500	34.53	0.112	125.82
RSB1000	27.31	0.092	134.76
RSB1500	26.62	0.087	135.42

Notes: SA = surface area, PV = pore volume, AP = the average pore diameter, RSB0 = 0 mL of K-sap enriched biochar, RSB500 = 500 mL of K-sap enriched biochar, RSB1000 = 1,000 mL of K-sap enriched biochar, and RSB1500 = 1,500 mL of K-sap enriched biochar.

FTIR of functional group

Figure 2 shows that the FTIR results of biochar enriched with 1,000 mL of K-sap kg^{-1} of biochar (RSB1000) have eight peak wave numbers, while the other volumes of 0 (RSB0), 500 (RSB500), and 1500 (RSB1500) mL of K-sap kg^{-1} biochar each have six peak numbers. In Figure 2, the increase in the volume of K-sap of peak waves in RSB1000 was detected in peak waves of 1,424.07 and 875.95 cm^{-1}. In addition, peak wave numbers with ranges of 3,405.70-3,445.29, 1,597.7-1,632.06, 1,384.39-1384.46, 1,092.84-1,096.81, 795.86-796.71, and 467.77-470.72 were detected for all biochar treatments.

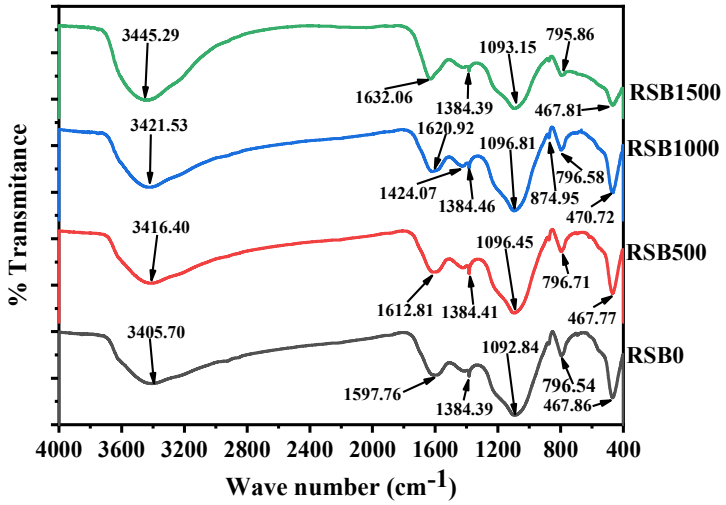

Figure 2. FTIR of functional group. Notes: RSB0 = 0 mL of K-sap enriched biochar, RSB500 = 500 mL of K-sap enriched biochar, RSB1000 = 1,000 mL of K-sap enriched biochar, and RSB1500 = 1,500 mL of K-sap enriched biochar.

The wave peaks of 1,424.07 cm^{-1} and 875.95 cm^{-1} with transmittance intensities of 57.799% and 88.465% were only seen in biochar RSB1000 (Table 3). Table 3 shows the transmittance intensity for the wave peak number range of 3,405.70-3,445.29 $cm^{-1,}$ and 467.77-470.72 cm^{-1} of the biochar treatment decreased with the increase in the volume of K-sap added sequentially from the highest intensity to the lowest according to the following sequential treatment, RSB0 > RSB500 > RSB1000 > RSB1500. The pattern of transmittance intensity change for the peak wave range of 1597.7-1632.06 cm^{-1} from RSB0 of 53.365% increased to 54.084% with the addition of 500 mL of K-sap, then the intensity decreased to below the precursor biochar intensity value (RSB0) with the addition of 1,000 and 1,500 mL of K-sap. For the range of wave numbers 1,384.39-1,384.46 cm^{-1}, the transmittance intensity of precursor biochar of 52.209% increased to 52.368% with the addition of 500 mL, 55.623% with 1,000 mL, on the contrary, decreased to below the precursor biochar value to 50.484% with the addition of 1,500 mL of K-sap. For the range of peak wave numbers of precursor biochar has a transmittance intensity of 9.999%, then the intensity is increased by 10.00% both with the addition of 500 (RSB500) and 1,000 mL of K-sap (RSB1000), then the addition of up to 1,500 mL of K-sap kg^{-1} biochar (RSB1500) decreases to the transmittance intensity of precursor biochar (RSB0).

Table 3. The wave absorbance intensity between the treatment of rice straw biochar enriched in volume is different from K-sap kg^{-1} biochar.

Range of peak wave number (cm^{-1})	Intensity of transmittance (%)				Functional group
	RSB0	RSB500	RSB1000	RSB1500	
3,405.70-3,445.29	44.106	42.138	35.301	18.813	Hydroxyl (–OH stretching) (Xiao et al., 2014)
1,597.7-1,632.06	53.365	54.084	52.192	41.804	Carbonyl (C-O) (Jindo et al., 2014)
1,424.07	-	-	57.799	-	Aliphatic (C-H deformation) (Nandiyanto et al., 2019; Benbi and Brar, 2021)
1,384.39-1,384.46	52.209	52.368	55.623	50.484	Stretching mode C-N or N–O stretching vibration from –NO2 groups (Yang et al., 2007; Castejón-del Pino et al., 2023)
1,092.84-1,096.81	9.999	10.000	10.000	9.999	Organic siloxane or silicone (Si-O-Si) (Nandiyanto et al., 2019)
875.95	-	-	88.465	-	Aromatic (C–H deformation or vibration band of aliphatic -C-C-C-H 1,3-Disubstitution) (Nandiyanto et al., 2019; Benbi and Brar, 2021)
795.86-796.71	74.019	76.338	75.202	45.632	Stretching vibration of Si-O (Shu et al., 2022)
467.77-470.72	28.889	31.313	29.500	13.522	Si-O/Si-C structures (Um-E-laila et al., 2021)

Notes: RSB0 = 0 mL of K-sap enriched biochar, RSB500 = 500 mL of K-sap enriched biochar, RSB1000 = 1,000 mL of K-sap enriched biochar, and RSB1500 = 1,500 mL of K-sap enriched biochar.

X-ray diffraction of enriched biochar

In Figure 3, the XRD pattern of all biochar treatments shows the crystal peaks. The most prominent peak intensity for all biochar occurs in the diffraction region (2 theta) of 20-30 degrees, followed by 35-50 degrees and 52-70 degrees. Figure 4 shows that the crystalline index of biochar precursor (RSB0) decreased with the increase in the volume of K-sap water. The crystallization index of K-sap enriched rice straw biochar decreased with increasing K-sap volume. The crystallization index of RSB0 was 44.95%, RSB500 was 42.48%, RSB1000 was 39.82%, and RSB1500 was 39.03%.

Water holding capacity and retention of soil

ANOVA results showed that rice straw biochar enriched with different volumes of K-sap had a significant effect (df 4; 8, F = 30.741 at p = 0.000) on soil water holding capacity (SWHC). SWHC occurred at B0 was the lowest and significantly different (LSD at p level <0.05) compared to rice straw biochar enriched with a different volume of K-sap. The difference in SWHC between RSB0, RSB500, RSB1000, and RSB1500 was not significant (p>0.5) according to the LSD test (Figure 5). Soil water holding capacity in RSB0 treatment was higher than that of control (B0), RSB500, RSB1000, and RSB1500. The day after the soil was saturated, the amount of water held at B0 was 43.50%. With the addition of RSB0, the amount of groundwater increased by 10% to 53.50%, RSB500 by 6.0% to 49.50%, and RSB1000 and RSB1500 by 8.33% to 51.83%, respectively. The amount of water retained in the control soil (B0) was 30% on the 14^{th} day after saturation, while with the addition of RSB0, the amount of water retained was 40%, RSB500 36.83%, RSB1000 38.50%, and RB1550 38.83%, respectively.

On the 24th day after saturation, the amount of water held in RSB0 decreased by 30%. RSB500, RSB1000, and RSB1500 decreased by 25.17%, 27.67%, and 27.50%, while B0 decreased by 18.17%. Additionally, the amount of water held in all soils was below 30% on the 28th day.

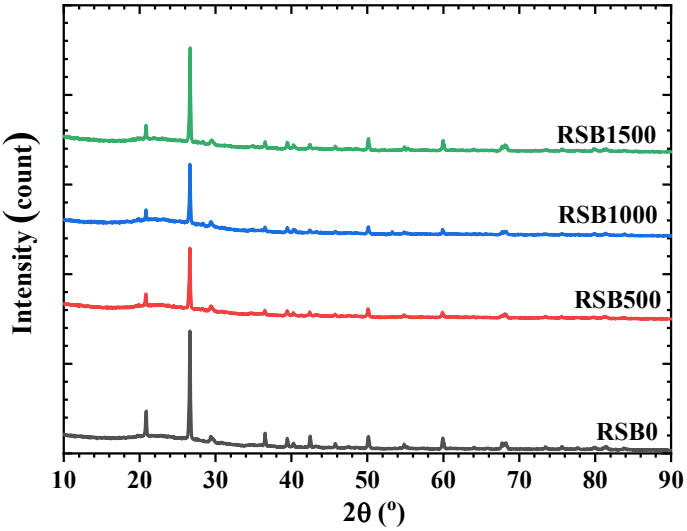

Figure 3. XRD pattern of rice straw biochar enriched with different volumes of K-sap. Notes: RSB0 = 0 mL of K-sap enriched biochar, RSB500 = 500 mL of K-sap enriched biochar, RSB1000 = 1,000 mL of K-sap enriched biochar, and RSB1500 = 1,500 mL of K-sap enriched biochar.

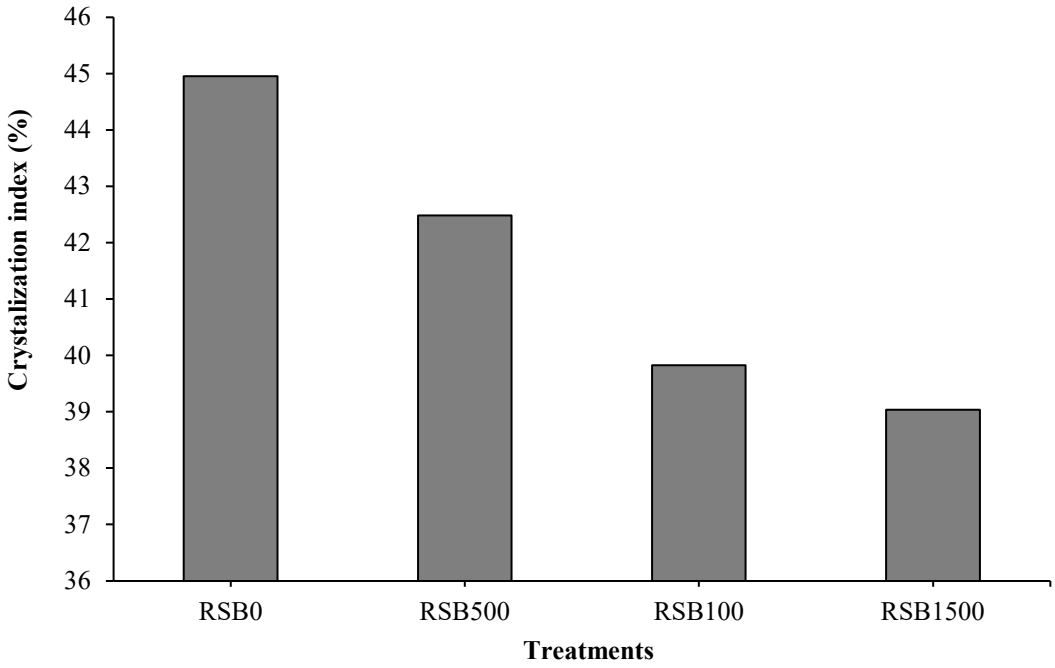

Figure 4. Changes in the crystallization index in biochar with an increase in K-sap volume. Notes: RSB0 = 0 mL of K-sap enriched biochar, RSB500 = 500 mL of K-sap enriched biochar, RSB1000 = 1,000 mL of K-sap enriched biochar, and RSB1500 = 1,500 mL of K-sap enriched biochar.

Soil aggregate distribution class size

The ANOVA results showed that the aggregate size class of 1-2 mm through dry sieving was significantly affected ($p<0.05$) by rice straw biochar enriched with a different volume from K-sap, while the other size class was not significant ($p>0.05$). In dry sifting, the proportion of aggregate class size 1-2 mm from the highest value drops to the lowest according to the following order: RSB1500 >RSB0 > RSB500 > RSB1000 > B0 (Table 4). The proportion of soil weight of 1-2 mm in RSB1500 compared to RSB500, RSB100, and B0 was significantly different (LSD at $p<0.05$) but not in RSB500. The proportion of weight

in RSB0 was significantly different compared to RSB1000 and B0, while compared to RSB500 was not significantly different. The difference in weight proportion in RSB500 compared to B0 was significant but not in RSB1000, and between RSB100 and B0 was not significantly different.

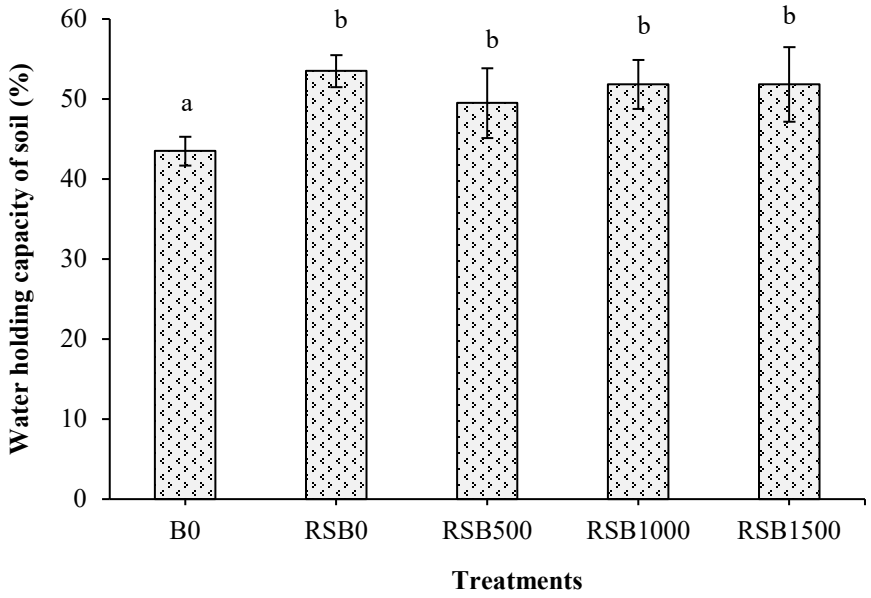

Figure 5. Differences in SWHC between rice straw biochar enriched with different volumes of K-sap. Different letters above the error bar indicate significantly different according to the LSD test at the $p<0.05$ level. Notes: RSB0 = 0 mL of K-sap enriched biochar, RSB500 = 500 mL of K-sap enriched biochar, RSB1000 = 1,000 mL of K-sap enriched biochar, and RSB1500 = 1,500 mL of K-sap enriched biochar.

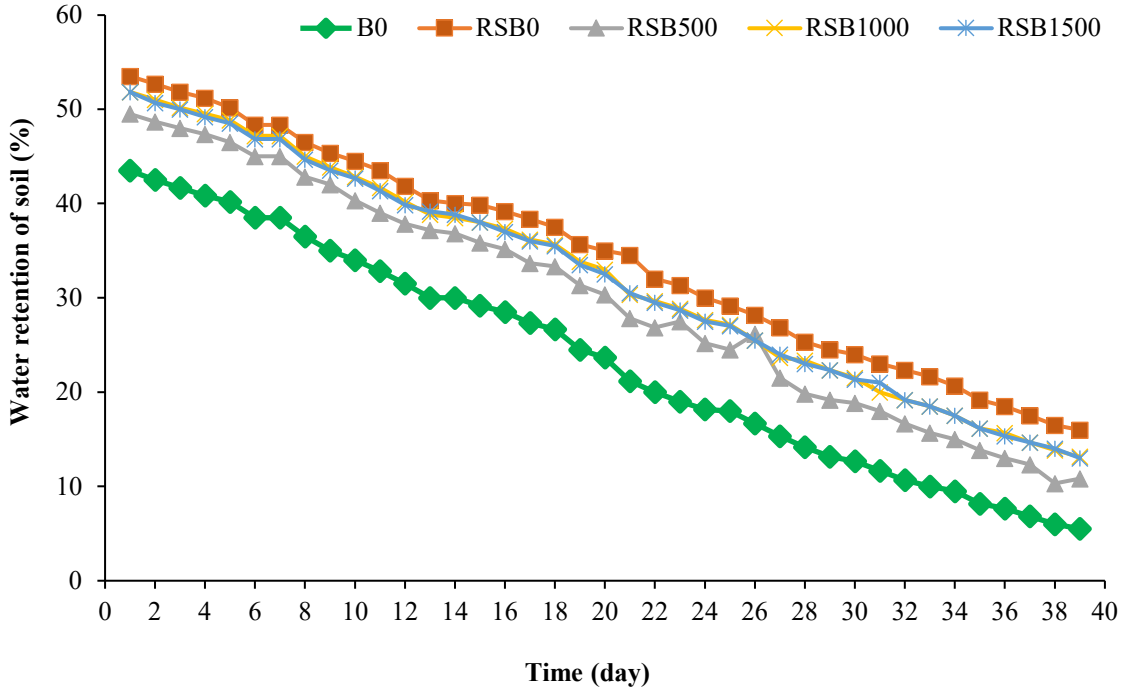

Figure 6. The capacity of soil water retention among rice straw biochar enriched with different volumes of K-sap. Notes: B0 = without biochar, RSB0 = 0 mL of K-sap enriched biochar, RSB500 = 500 mL of K-sap enriched biochar, RSB1000 = 1,000 mL of K-sap enriched biochar, and RSB1500 = 1,500 mL of K-sap enriched biochar.

Table 4. Difference in proportion (% ± s.d., n=3) weight of soil aggregate of different size classes between the treatment of rice straw biochar enriched in different volumes of K-sap kg^{-1} biochar on dry and wet sifting.

Treatments	Distribution of soil size aggregate class				
	<0.25 mm	0.25-1 mm	1-2 mm	2-4 mm	>4 mm
Dry sieving method					
B0	14.40±7.42 a	29.19±8.03 a	17.59±7.53 a	13.29±7.27 a	25.53±19.78 a
RSB0	18.34±11.68 a	41.73±6.97 a	24.02±1.68 cd	11.45±3.54 a	4.47±1.76 a
RSB500	22.47±10.81 a	41.02±10.10 a	23.43±1.31 bc	10.05±0.64 a	3.03±2.11 a
RSB1000	35.88±6.76 a	29.90±14.78 a	19.98±1.95 ab	11.43±8.20 a	2.82±1.61 a
RSB1500	18.53±8.25 a	40.74±9.11 a	27.07±1.07 d	9.81±2.60 a	3.86±2.21 a
Wet sieving method					
B0	71.86±5.32 a	20.52±4.13 a	5.60±1.45 a	1.93±0.68 a	0.10±0.04 a
RSB0	58.89±3.13 a	26.27±3.62 a	7.45±2.05 a	2.23±0.57 a	3.07±1.40 a
RSB500	53.43±9.25 a	29.39±5.00 a	11.06±3.22 a	2.43±1.08 a	3.68±3.06 a
RSB1000	48.38±15.55 a	28.56±2.66 a	6.60±2.22 a	2.52±0.81 a	13.94±18.86 a
RSB1500	57.43±11.27 a	29.25±8.21 a	5.26±0.58 a	1.34±0.80 a	6.72±10.04 a

Note: Numbers in the same column followed by different letters indicate the significant difference according to LSD test at p<0.05, B0 = without biochar, RSB0 = 0 mL of K-sap enriched biochar, RSB500 = 500 mL of K-sap enriched biochar, RSB1000 = 1,000 mL of K-sap enriched biochar, and RSB1500 = 1,500 mL of K-sap enriched biochar.

Soil aggregate stability indices

Table 5 shows that the difference in the index value of soil aggregate stability for both size classes of 0.25-1 mm, 1-2 mm, 2-4 mm, and >4 mm were not significant.

Soil respiration

Figure 7 shows that the amount of CO_2 released from the soil has continued to decline since days 14th, 28 th, 42 th, 56 th, and 70 th for all treatments. In the control soil (B0), the amount of CO_2 released was higher than that of other treatments during the incubation period. The level of CO_2 amount, regardless of the most, decreased to the least on the 14 th, 28 th, 56 th, and 70 th days according to the treatment, respectively, were B0 > RSB0 > RSB500 > RSB1000 > RSB1500.

Table 6 shows that the power function of the relationship between CO_2 release and time shows that the soil respiration rate occurred fastest in RSB500 at 1.15 mg CO_2 day^{-1}, sequentially the slowest occurred at RSB1000 of 1.09, RSB1500 of 1.05, B0 of 1.04 mg, and RSB0 of 1.01 mg CO_2 day^{-1}.

Table 5. The value of the soil aggregate stability index (value ± s.d., n = 3) of different size classes between the biochar treatment of rice straw enriched with different volumes of K-sap kg^{-1} biochar.

Treatment	Aggregate stability index			
	0.25-1 mm	1-2 mm	2-4 mm	>4 mm
B0	49.91±10.66 a	13.47±3.39 a	4.66±1.62 a	0.13±0.10 a
RSB0	64.61±9.18 a	18.04±5.34 a	5.56±1.49 a	12.14±8.00 a
RSB500	72.76±12.82 a	26.88±7.81 a	5.98±2.62 a	9.07±7.54 a
RSB1000	70.81±6.59 a	16.01±5.42 a	6.17±1.94 a	34.17±47.59 a
RSB1500	72.25±21.29 a	12.82±1.11 a	3.21±1.99 a	16.66±24.96 a

Notes: Numbers in the same column followed by different letters indicate a significant difference according to the LSD test at p<0.05, B0 = without biochar, RSB0 = 0 mL of K-sap enriched biochar, RSB500 = 500 mL of K-sap enriched biochar, RSB1000 = 1,000 mL of K-sap enriched biochar, and RSB1500 = 1,500 mL of K-sap enriched biochar.

Table 6. The power function was related to soil respiration (mg CO_2 -release 100 g^{-1} soil) and time (day) in each treatment of rice straw biochar enriched with different volumes of K-sap.

Treatment	Formula	R^2	Sig.
B0	$SR = (258.628\pm70.738)^{(-1.037\pm0.075)/day}$	0.936	0.000
RSB0	$SR = (183.319\pm36.507)^{(-1.011\pm0.055)/day}$	0.963	0.000
RSB500	$SR = (272.021\pm106.062)^{(-1.155\pm0.107)/day}$	0.892	0.000
RSB1000	$SR = (226.349\pm43.694)^{(-1.091\pm0.053)/day}$	0.968	0.000
RSB1500	$SR = (195.111\pm35.086)^{(-1.055\pm0.049)/day}$	0.970	0.000

Notes: SR is soil respiration, which is expressed by the amount of CO_2 released from the soil, B0 = without biochar, RSB0 = 0 mL of K-sap enriched biochar, RSB500 = 500 mL of K-sap enriched biochar, RSB1000 = 1,000 mL of K-sap enriched biochar, and RSB1500 = 1,500 mL of K-sap enriched biochar.

During 70 days of incubation, the rice straw biochar enriched with different volumes of K-sap had a significant effect on the total CO_2 released from the acidic soil. The highest and lowest total CO_2 released occurred in B0 (145.57±7.84 mg of CO_2 g^{-1} soil) and RSB500 (116.53 ± 6.52 CO_2 g^{-1} soil), respectively. The difference in total CO_2 released in RSB500 compared to B0 was significant but was not significant compared to other treatments. The result obtained between RSB0, RSB1000, and RSB1500 was not significantly different but was significantly different for the three treatments compared to B0 (Figure 8).

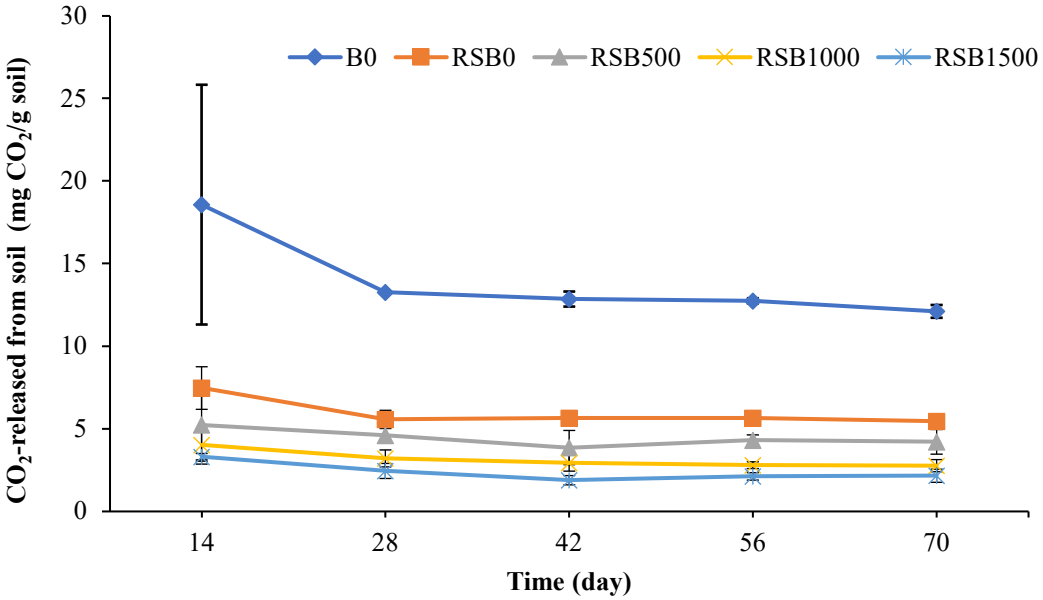

Figure 7. The pattern of CO_2 release from soil among rice straw biochar enriched with different volumes of K-sap. Notes: B0 = without biochar, RSB0 = 0 mL of K-sap enriched biochar, RSB500 = 500 mL of K-sap enriched biochar, RSB1000 = 1,000 mL of K-sap enriched biochar, and RSB1500 = 1,500 mL of K-sap enriched biochar.

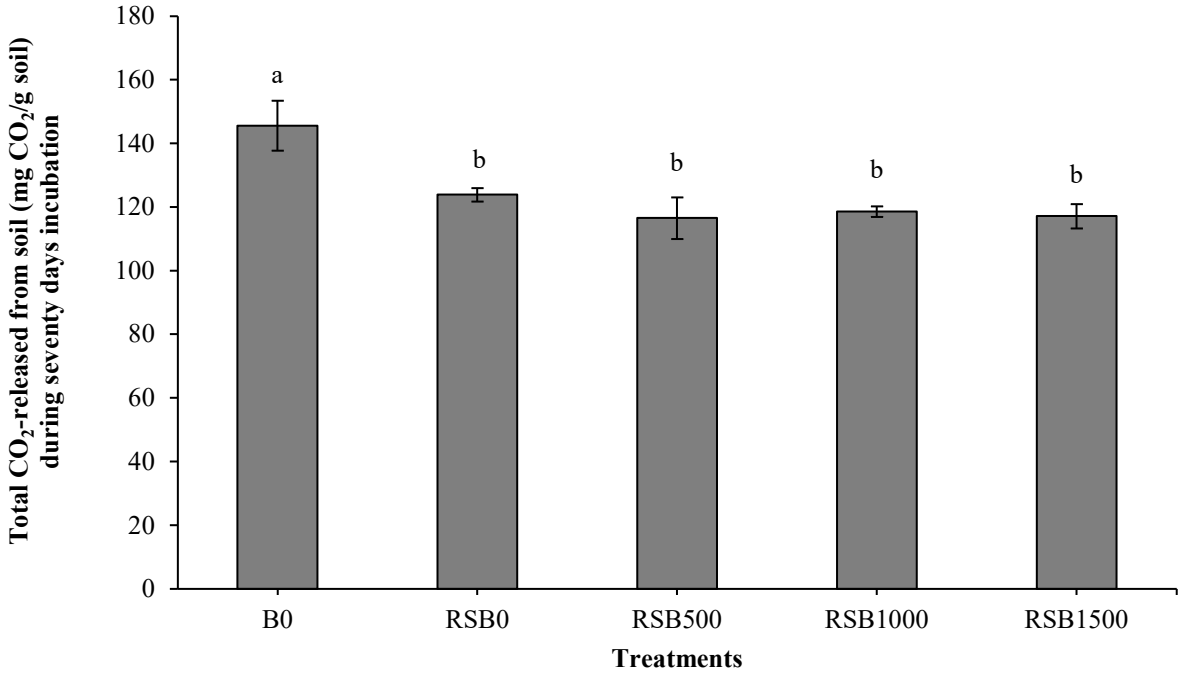

Figure 8. Total CO_2 released from the soil treated with rice straw biochar enriched with different volumes of K-sap during seven days of incubation. Notes: B0 = without biochar, RSB0 = 0 mL of K-sap enriched biochar, RSB500 = 500 mL of K-sap enriched biochar, RSB1000 = 1,000 mL of K-sap enriched biochar, and RSB1500 = 1,500 mL of K-sap enriched biochar.

Chemical characteristics of soil

The ANOVA results showed that pH (H_2O), pH (KCl), organic C, total N, $Al^{3+,}$ and H^+ were significantly ($p<0.05$) affected by the treatment, but not for C: N ratio and cation exchangeable capacity (CEC). According to Table 7, there was a significant difference (LSD at $p<0.05$) between pH (H_20) and pH (KCl) under all enriched rice straw biochar compared to no biochar (B0). Meanwhile, the biochar without and with enriched volumes of K-sap was not significant. The organic C content of soil from the highest to the lowest was decreased according to RSB15000 > RSB0 > RSB1000 > RSB500. The difference between RSB1500 compared to others was significant (LSD at $p<0.05$), while RSB0, RSB1000, and RSB500 were not significant (LSD at $p>0.05$).

Table 7. Differences in parameters of soil chemical characters after incubation with treatment,

Parameter	Treatment				
	B0	RSB0	RSB500	RSB1000	RSB1500
pH (H_2O)	4.40±0.10 a	6.03±0.38 b	6.37±0.42 b	6.13±0.06 b	6.27±0.46 b
pH (KCl)	3.83±0.06 a	5.43±0.46 b	5.90±0.36 b	5.70±0.10 b	5.87±0.38 b
Organic C	1.19±0.07 a	1.79±0.13 b	1.77±0.15 b	1.78±0.12 b	2.11±0.05 c
Total N	0.11±0.01 a	0.16±0.01 b	0.15±0.01 b	0.16±0.01 b	0.17±0.01 c
C: N-ratio	11.00±0.00 a	11.67±0.58 a	11.67±0.58 a	11.67±0.58 a	12.00±0.00 a
P_2O_5-Bray (ppm)	15.30±3.08 a	113.53±9.05 b	139.43±52.80 b	127.40±25.38 b	130.63±16.38 b
Avail. P_2O_5-Olsen (ppm)	19.00±1.00 a	68.00±7.55 b	66.00±4.00 b	67.67±7.23 b	71.00±3.00 b
Available K_2O-Morgan ($x10^2$ ppm)	1.54±0.22 a	15.41±6.45 b	21.91±2.57c	21.31±2.59c	24.56±0.89c
Exch. Ca ($cmol_c. kg^{-1}$)	1.57±0.20 a	3.81±0.15 b	3.64±0.22 b	4.68±0.15 c	4.58±0.15 c
Exch. Mg ($cmol_c. kg^{-1}$)	0.45±0.04 a	1.21±0.11 b	1.15±0.08 b	1.41±0.11 c	1.37±0.14 c
Exch. K ($cmol_c. kg^{-1}$)	0.27±0.06 a	3.17±1.00 b	4.66±0.10 c	4.47±0.14 c	4.78±0.21 c
Exch. Na ($cmol_c. kg^{-1}$)	0.51±0.09 a	0.76±0.24 a	0.88±0.29 a	0.94±0.24 a	1.03±0.18 a
CEC ($cmol_c. kg^{-1}$)	9.61±0.50 a	9.36±0.19 a	9.78±0.32 a	9.23±0.20 a	9.95±0.42 a
Base saturation (%)	29.33±3.06 a	94.33±9.81 b	100.00±0.00 b	100.00±0.00 b	100.00±0.00 b
Al^{3+} ($cmol_c. kg^{-1}$)	1.85±0.34 a	0.00±0.00 b	0.00±0.00 b	0.00±0.00 b	0.00±0.00 b
H^+ ($cmol_c. kg^{-1}$)	0.73±0.07 a	0.34±0.06 b	0.31±0.02 b	0.36±0.03 b	0.35±0.08 b

Notes: Numbers in the same line followed by different letters indicate a significant difference according to LSD at $p<0.05$, B0 = without biochar, RSB0 = 0 mL of K-sap enriched biochar, RSB500 = 500 mL of K-sap enriched biochar, RSB1000 = 1,000 mL of K-sap enriched biochar, and RSB1500 = 1,500 mL of K-sap enriched biochar

Table 7 shows that the highest and lowest total N in soil occurs in RSB1500 and B0, respectively. The levels of total N content in the soil ranged from the highest to the lowest according to the treatment, including RSB1500 > RSB100 = RSB0 > RSB500 > B0. The difference in total N between RSB1500 compared to others was significant. Similarly, the total N content between RSB0, RSB1000, and RSB500 was not significantly different, but it was different compared to B0. The Al^{3+} ions were only detected in the image SEM (Figure 1a) of B0 and were significantly different (LSD at $p<0.05$) compared to other treatments. The difference in H^+ ion levels between RSB0, RSB500, RSB1000, and RSB1500 was not significant. The order of H^+ ion levels in the soil decreased from the highest to the lowest according to B0 > RSB1000 > RSB1500 > RSB0 > RSB500.

Discussion

SEM image (Figure 1a) showed the surface morphology of the enriched rice straw biochar used. There were surface pores available as the adsorption area of K-sap, consisting of macropores, micropores, and ultramicropores (Yang et al., 2021). In this research, rice straw biochar was produced at a temperature of 320 ºC. The pores created in the pyrolysis temperature range of 300-400 ºC were dominated by micropore areas, which are positively correlated with BET (Phuong et al., 2016). Figures 1b, 1c, and 1d show that the surface area after enrichment was covered with gel droplets from K-sap and expanded with the increase in volume. Polysaccharides and film-like layers covering the surface area of the biochar pores are found in K-sap (Sudhakar et al., 2021; Kilowasid et al., 2023; Kilowasid et al., 2024). The film layer allows the distribution of the size and surface volume of the biochar to change. After the addition of K-sap and the reduction rate increased with the volume, the surface area of the biochar precursor (RSB0) decreased. In this context, the mycopoeial dominance of the biochar area was eroded by the cover of the drying K-sap film layer. Table 2 shows a decrease in pore volume in the addition of 1000 and 1500 mL of K-sap kg^{-1} biochar. These results report more K-sap droplets covering pores, especially micropores from the biochar surface. The increase in pore volume after the addition of 500 mL K-sap may be related to several micro- and meso-pores from the biochar. The average pore radius increases with the addition of K-sap volume.

The presence of a layer of K-sap film covering the surface of the biochar contributes to the change in the transmittance intensity and wave bandwidth

(Kilowasid et al., 2023). Meanwhile, the addition of 1,000 mL K-sap kg^{-1} biochar forms 1,424.07 cm^{-1} and 875.95 cm^{-1} peak wave numbers in the FTIR spectrum related to the aliphatic and aromatic functional groups with an intensity of 57.78% and 88.45%, respectively. The appearance of the two clusters shows the participation and interaction between biochar and K-sap (Elsupikhe et al., 2015) at a volume of 1,000 mL. K-sap contains rich carbonyl and hydroxyl groups from carbohydrates (Masarin et al., 2016). The aliphatic and aromatic functional groups originate from C-H deformation due to the strength of the CH_3 interaction from straw biochar with CH_3 of K-sap at 1,000 mL (Yew et al., 2016). The aromatic groups are also obtained from the substitution of K-sap with rice straw biochar. In this context, the C and H bonds can break due to the strength of the interaction to form a new functional group (Arnaut, 2021). The breaking of the C bond causes a certain amount of carbon to be released into the atmosphere in the form of CO_2 (Chang et al., 2023). Therefore, the proportion of carbon decreased by 0.23 times compared to the precursor biochar (Table 1).

The changes in pores, areas, and functional groups of the biochar surface affected the role of improving the quality of acidic soil (Hafeez et al., 2022; Kilowasid et al., 2024). Therefore, the soil capacity of water storage in biochar with and without K-sap increased by 1.14-1.23 times. The events are related to the porosity and surface area of the biochar (Batista et al., 2018). This is because the surface area of unenriched biochar is wider than the enriched counterpart, as shown in Table 2. In this context, the hydroxyl (-OH) and carbonyl (C-O) functional groups from the surface of unenriched biochar are more available due to the breaking of hydrogen bonds from the cellulose of rice straw. From the FTIR analysis, the transmittance intensity of unenriched biochar was stronger than the biochar enriched with K-sap (Table 2). This decrease in intensity is related to polymerization due to the addition of K-sap-containing rich polysaccharides (Munajad et al., 2018; Bhuyar et al., 2021). Hydrophilic- COOH, -OH, and C-O functional groups of the biochar surface increase the water-holding capacity of the soil (Dengxiao et al., 2024). From the presence of the hydrophilic group, the application of biochar may increase the capacity of acidic soils to hold water (Figure 5).

The capacity to hold water is controlled by the structure and aggregation of the soil (Kelly et al., 2017). Different sizes of aggregates are formed from the fraction of sand, silt, and clay particles bound (Amelung et al., 2023). The aggregates can be improved using soils with fine texture (Wagner et al., 2007). The formation of 0.25-2 mm size grade macro aggregates is increased by organic C derived from biochar (Jin et al., 2020). A fraction of 11% sand particles, 61% silt, and 28% clay grouped into fine texture soil. The formation of soil aggregates grade size 1-2 mm was also increased by the addition of rice straw biochar enriched with different volumes of K-sap. Under dry conditions, biochar plays an important role in the formation of aggregates from finely textured soils (Pituello et al., 2018). For wet sifting conditions, the 1-2 mm deep size grade macroaggregate formed was degraded into aggregates dominated by the size class of <0.25 mm. An index was also formed from the aggregate stability of 1-2 mm macroaggregates through the addition of biochar enriched with various volumes of K-sap. The soil particle fractions do not have strong bonds in the formation of aggregates during the incubation period. The value of the index decreases with the increase in the volume of K-sap, causing rice straw biochar to become more amorphous. The contribution of K-sap with amorphous properties and high solubility in water leads to an increase in percentage (Ferdiansyah et al., 2023). Microaggregates with high solubility are formed from soil with macroaggregates.

The total C in soil aggregates emitted in the form of CO_2 is increased through biochar (Fungo et al., 2017; El-Naggar et al., 2018), which contains a recalcitrant fraction. This fraction is resistant to decomposition due to the increased accumulation of organic C (Zheng et al., 2022). The CO_2 released 14 days after incubation without biochar decreased more drastically. Therefore, organic C enriched with a volume of 1,500 mL has recalcitrant characteristics and was increased by 1.5 times using rice straw biochar. The addition of K-sap volume to enrich biochar forms soil organic C as a target of biological respiration activity, and the increased amount results in a higher rate of CO_2 release (Zhang et al., 2024). According to Table 6, the addition of biochar without enrichment had the smallest constant value rate of CO_2 release, in line with Wang et al. (2023). The K-sap enriched biochar has a release constant rate of CO_2 higher than those without K-sap enrichment. The CO_2 release rate coefficient is related to the water-soluble decomposing properties of K-sap (Martiny et al., 2020). Even though the constant discharge rate in enriched biochar K-sap is higher, the total CO_2 released from acidic soil during seventy days of incubation was relatively lower. Therefore, the addition of biochar efficiently increases the amount of organic C stored in acidic soils (Li et al., 2024). K-sap contains nitrogen from proteins which can be dissolved in water (Kumar et al., 2014). The use of biochar with nitrogen content increases the level of the nutrient through the reduction of soil mineral loss (Gao et al., 2022). In this research, the enrichment increased the performance of total soil nitrogen biochar (Table 7) since K-sap contains the nutrients released into the soil (Kilowasid et al., 2023).

The addition of enriched biochar with different volumes of K-sap increased up to ± 2 units of pH from acidic soil. The increase was relatively higher than that of no enriched soil, as shown in Table 6. This was reported by the content of K, Ca, Mg, and Na in K-sap enriched biochar compared to unenriched.The base

cations in a biochar-soil mixture were increased by the content of K, Ca, Mg, and Na in biochar (Adhikari et al., 2024). The concentration of K^+, Ca^{2+}, and Mg^{2+} ions was increased using k-sap enriched biochar. The concentration of H^+ and Al^{3+} ions was reduced, while the saturation of soil alkalinity was increased. The presence of hydroxyl (-OH) groups on the surface of biochar without or with enriched K-sap plays an important role in the adsorption of H^+ and Al^{3+} ions to form Al-OH complexes (Song et al., 2019; Li et al., 2023).

Conclusion

In conclusion, the ratio of K-sap volume to biochar weight was reported to change the surface area and form new wave peak numbers of carbon deformation. The surface area and pore size of biochar increased, while the pore volume and crystallinity decreased with the addition of K-sap volume. This change in character affected the performance of biochar in improving the capacity of the soil to retain water and store carbon. The composition of soil aggregate size, total N levels, available P and K, and the base cations were interchangeable. Conversely, the amount of CO_2 released and the concentration of Al^{3+} ions could be reduced in the soil solution of acidic soils.

Acknowledgments

This research received funding from the Superior Applied Research Scheme of Higher Education with contract No. 270/E4.1/AK.04.PT/2021. The author is grateful to the Directorate of Resources, Directorate General of Higher Education, Culture, Research and Technology of the Republic of Indonesia. In addition, the author also extended thanks to the National Research and Innovation Agency (BRIN) Laboratory for testing materials using FTIR and X-ray and ITS Mechanical Engineering Laboratory for SEM-EDS.

References

Adhikari, S., Moon, E. and Timms, W. 2024. Identifying biochar production variables to maximize exchangeable cations and increase nutrient availability in soils. *Journal of Cleaner Production* 446:141454, doi:10.1016/j.jclepro.2024.141454.

Amelung, W., Meyer, N., Rodionov, A., Knief, C., Aehnelt, M., Bauke, S.L., Biesgen, D., Dultz, S., Guggenberger, G., Jaber, M., Klumpp, E., Kögel-Knabner I., Nischwitz, V., Schweizer, S.A., Wu B., Totsche, K.U. and Lehndorff, E. 2023. Process sequence of soil aggregate formation disentangled through multi-isotope labelling. *Geoderma* 429, doi:10.1016/j.geoderma.2022.116226.

Arnaut, L. 2021. *Chemical Kinetics: From Molecular Structure to Chemical Reactivity*. Second Edittion, Elsevier, doi:10.1016/B978-0-444-64039-0.00026-1.

Audette, Y., Congreves, K.A., Schneider, K., Zaro, G.C., Nunes, A.L.P., Zhang, H. and Voroney, R.P. 2021. The effect of agroecosystem management on the distribution of C functional groups in soil organic matter: a review. *Biology and Fertility of Soils* 57(7):881-894, doi:10.1007/s00374-021-01580-2.

Bajpai, S., Shukla, P.S., Prithiviraj, B., Critchley, A.T. and Nivetha, N. 2024. Editorial: development of next generation bio stimulants for sustainable agriculture. *Frontiers in Plant Science* 15:8-10, doi:10.3389/fpls.2024.1383749.

Baquy, M.A.-A., Li, J., Jiang, J., Mehmood, K., Shi, R.-Y. and Xu, R.-K. 2018. Critical pH and exchangeable Al of four acidic soils derived from different parent materials for maize crops. *Journal of Soils and Sediments* 18, doi:10.1007/s11368-017-1887-x.

Basheer, S., Wang, X., Farooque, A.A., Nawaz, R.A., Pang, T. and Neokye, E.O. 2024. A review of greenhouse gas emissions from agricultural soil. *Sustainability* 16(11):1-18, doi:10.3390/su16114789.

Batista, E.M.C.C., Shultz, J., Matos, T.T.S., Fornari, M.R., Ferreira, T.M., Szpoganicz, B., De Freitas, R.A. and Mangrich, A.S. 2018. Effect of surface and porosity of biochar on water holding capacity aiming indirectly at preservation of the Amazon biome. *Scientific Reports* 8(1):1-9, doi:10.1038/s41598-018-28794-z.

Benbi, D.K. and Brar, K. 2021. Pyrogenic conversion of rice straw and wood to biochar increases aromaticity and carbon accumulation in soil. *Carbon Management* 12(4):385-397, doi:10.1080/17583004.2021.1962409.

Bhuyar, P., Sundararaju, S., Rahim, M.H.A., Unpaprom, Y., Maniam, G.P. and Govindan, N. 2021. Antioxidative study of polysaccharides extracted from red (*Kappaphycus alvarezii*), green (*Kappaphycus striatus*) and brown (*Padina gymnospora*) marine macroalgae/seaweed. *SN Applied Sciences* 3(4):1-9, doi:10.1007/s42452-021-04477-9.

Bolan, N., Sarmah, A.K., Bordoloi, S., Bolan, S., Padhye, L.P., Van Zwieten, L., Sooriyakumar, P., Khan, B.A., Ahmad, M., Solaiman, Z.M., Rinklebe, J., Wang, H., Singh, B.P. and Siddique, K.H.M. 2023. Soil acidification and the liming potential of biochar. *Environmental Pollution* 317, doi:10.1016/j.envpol.2022.120632.

Castejón-del Pino, R., Cayuela, M.L., Sánchez-García, M. and Sánchez-Monedero, M.A. 2023. Nitrogen availability in biochar-based fertilizers depending on activation treatment and nitrogen source. *Waste Management* 158:76-83, doi:10.1016/j.wasman.2023.01.007.

Chang, B., Pang, H., Raziq, F., Wang, S., Huang, K.W., Ye, J. and Zhang, H. 2023. Electrochemical reduction of carbon dioxide to multicarbon (C_{2+}) products: challenges and perspectives. *Energy and Environmental Science* 16(11):4714-4758, doi:10.1039/d3ee00964e.

Cheng, X., Han, H., Zhu, J., Peng, X., Li, B., Liu, H. and Epstein, H. 2021. Forest thinning and organic matter manipulation drives changes in soil respiration in a *Larix principis-rupprechtii* plantation in China. *Soil and Tillage Research* 211:104996, doi:10.1016/j.still.2021.104996.

Chew, K.W., Chia, S.R., Yen, H.W., Nomanbhay, S., Ho, Y.C. and Show, P.L. 2019. Transformation of biomass waste into sustainable organic fertilizers. *Sustainability* 11(8), doi:10.3390/su11082266.

Dengxiao, Z., Hongbin, J., Wenjing, Z., Qingsong, Y., Zhihang, M., Haizhong, W., Wei, R., Shiliang, L. and Daichang, W. 2024. Combined biochar and water-retaining agent application increased soil water retention capacity and maize seedling drought resistance in

Fluvisols. *Science of The Total Environment* 907:167885, doi:10.1016/j.scitotenv.2023.167885.

Don, A., Seidel, F., Leifeld, J., Kätterer, T., Martin, M., Pellerin, S., Emde, D., Seitz, D. and Chenu, C. 2024. Carbon sequestration in soils and climate change mitigation—Definitions and pitfalls. *Global Change Biology* 30(1), doi:10.1111/gcb.16983.

El-Naggar, A., Awad, Y.M., Tang, X.Y., Liu, C., Niazi, N.K., Jien, S.H., Tsang, D.C., Song, H., Ok, Y.S. and Lee, S.S. 2018. Biochar influences soil carbon pools and facilitates interactions with soil: A field investigation. *Land Degradation and Development* 29(7):2162-2171, doi:10.1002/ldr.2896.

Elsupikhe, R.F., Shameli, K., Ahmad, M.B., Ibrahim, N.A. and Zainudin, N. 2015. Green sonochemical synthesis of silver nanoparticles at varying concentrations of κ-carrageenan. *Nanoscale Research Letters* 10(1):1-8, doi:10.1186/s11671-015-0916-1.

Enaime, G. and Lübken, M. 2021. Agricultural waste-based biochar for agronomic applications. *Applied Sciences* 11(19), doi:10.3390/app11198914.

Fadilah, S., Alimuddin, Pong-Masak, P.R., Santoso, J. and Parenrengi, A. 2016. Growth, morphology and growth related hormone level in *Kappaphycus alvarezii* produced by mass selection in Gorontalo waters, Indonesia. *HAYATI Journal of Biosciences* 23(1):29-34, doi:10.1016/j.hjb.2015.09.004.

FAO. 2023. Global soil laboratory network. Standard Operating Procedures for Soil Moisture Content by Gravimetric Method.

Ferdiansyah, R., Abdassah, M., Zainuddin, A., Rachmaniar, R. and Chaerunisaa, A.Y. 2023. Effects of alkaline solvent type and pH on solid physical properties of carrageenan from *Eucheuma cottonii*. *Gels* 9(5), doi:10.3390/gels9050397.

Fungo, B., Lehmann, J., Kalbitz, K., Thiongo, M., Okeyo, I., Tenywa, M. and Neufeldt, H. 2017. Aggregate size distribution in a biochar-amended tropical Ultisol under conventional hand-hoe tillage. *Soil and Tillage Research* 165:190-197, doi:10.1016/j.still.2016.08.012.

Gao, Y., Fang, Z., Van Zwieten, L., Bolan, N., Dong, D., Quin, B.F., Meng, J., Li, F., Wu, F., Wang, H. and Chen, W. 2022. A critical review of biochar-based nitrogen fertilizers and their effects on crop production and the environment. *Biochar* 4(1):1-19, doi:10.1007/s42773-022-00160-3.

Ghorbani, M., Asadi, H. and Abrishamkesh, S. 2019. Effects of rice husk biochar on selected soil properties and nitrate leaching in loamy sand and clay soil. *International Soil and Water Conservation Research* 7(3):258-265, doi:10.1016/j.iswcr.2019.05.005.

Grados, D., Kraus, D., Haas, E., Butterbach-Bahl, K., Olesen, J.E. and Abalos, D. 2024. Common agronomic adaptation strategies to climate change may increase soil greenhouse gas emission in Northern Europe. *Agricultural and Forest Meteorology* 349, doi:10.1016/j.agrformet.2024.109966.

Hafeez, A., Pan, T., Tian, J. and Cai, K. 2022. Modified biochars and their effects on soil quality: A review. *Environments* 9(5), doi:10.3390/environments9050060.

Halder, M., Ahmad, S.J., Rahman, T., Joardar, J.C., Siddique, M.A.B., Islam, M.S., Islam, M.U., Liu, S., Rabbi, S. and Peng, X. 2023. Effects of straw incorporation and straw-burning on aggregate stability and soil organic carbon in a clay soil of Bangladesh. *Geoderma Regional* 32:e00620, doi:10.1016/j.geodrs.2023.e00620.

Islam, M.U., Jiang, F., Guo, Z. and Peng, X. 2021. Does biochar application improve soil aggregation? A meta-analysis. *Soil and Tillage Research* 209:104926, doi:10.1016/j.still.2020.104926.

Jamilatun, S., Pitoyo, J., Amelia, S., Ma'arif, A., Hakika, D.C. and Mufandi, I. 2022. Experimental study on the characterization of pyrolysis products from bagasse (*Saccharum officinarum* L.): Bio-oil, biochar, and gas products. *Indonesian Journal of Science and Technology* 7(3):565-582, doi:10.17509/ijost.v7i3.51566.

Jiang, J., Wang, Y.P., Yu, M., Cao, N. and Yan, J. 2018. Soil organic matter is important for acid buffering and reducing aluminum leaching from acidic forest soils. *Chemical Geology* 501:86-94, doi:10.1016/j.chemgeo.2018.10.009.

Jin, L., Wei, D., Yin, D., Zhou, B., Ding, J.L., Wang, W., Zhang, J., Qiu, S., Zhang, C., Li, Y., An, Z., Gu, J. and Wang, L. 2020. Investigations of the effect of the amount of biochar on soil porosity and aggregation and crop yields on fertilized black soil in northern China. *PLoS ONE* 15:1-15, doi:10.1371/journal.pone.0238883.

Jindo, K., Mizumoto, H., Sawada, Y., Sanchez-Monedero, M.A. and Sonoki, T. 2014. Physical and chemical characterization of biochars derived from different agricultural residues. *Biogeosciences* 11(23):6613–6621, doi:10.5194/bg-11-6613-2014.

Jones, D.L., Prabowo, A.M. and Kochian, L.V. 1996. Aluminium-organic acid interactions in acid soils. *Plant and Soil* 182(2):229-237, doi:10.1007/BF00029054.

Kelly, C.N., Benjamin, J., Calderón, F.C., Mikha, M.M., Rutherford, D.W. and Rostad, C.E. 2017. Incorporation of biochar carbon into stable soil aggregates: the role of clay mineralogy and other soil characteristics. *Pedosphere* 27(4):694-704, doi:10.1016/S1002-0160(17)60399-0.

Kilowasid, L.M.H., Alam, S., Rakian, T.C., Ansar, N.A., Nurfadillah, Ramdan, N.H., Jaya, I., Suryana, Agustin, W., Rahni, N.M., Mashuni, and Safuan, L.O. 2024. Effect of cogon grass biochar enriched with nitrogen fertilizer dissolved in seaweed liquid extract on soil water content of Ultisol. *Journal of Degraded and Mining Lands Management* 11(3): 5585-5596, doi:10.15243/jdmlm.2024.113.5585.

Kilowasid, L.M.H., Manik, D.S., Nevianti, Komang, G.A., Mutmainna, P., Afa, L.O., Rakian, T.C., Hisein, W.S.A., Ramadhan, L.O.A.N. and Alam, S. 2023. The quality of acid soils treated with seaweed (*Kappapychus alvarezii*) sap enriched biochar from Southeast Sulawesi, Indonesia. *Journal of Degraded and Mining Lands Management* 10(2):4255-4269, doi:10.15243/jdmlm.2023.102.4255.

Kumar, K., Ganesan, K., Selvaraj, K. and Subba Rao, P.V. 2014. Studies on the functional properties of protein concentrate of *Kappaphycus alvarezii* (Doty) Doty - an edible seaweed. *Food Chemistry* 153:353-360, doi:10.1016/j.foodchem.2013.12.058.

Li, B., Guo, Y., Liang, F., Liu, W., Wang, Y., Cao, W., Song, H., Chen, J. and Guo, J. 2024. Global integrative meta-analysis of the responses in soil organic carbon stock to biochar amendment. *Journal of Environmental Management* 351:119745, doi:10.1016/j.jenvman.2023.119745.

Li, K-w., Lu, H-l., Nkoh, J.N. and Xu, R-k. 2023. The important role of surface hydroxyl groups in aluminum activation during phyllosilicate mineral acidification. *Chemosphere* 313:137570, doi:10.1016/j.chemosphere.2022.137570.

Liu, G., Dai, Z., Liu, X., Dahlgren, R.A. and Xu, J. 2022. Modification of agricultural wastes to improve sorption capacities for pollutant removal from water – a review. *Carbon Research* 1(1):1-24, doi:10.1007/s44246-022-00025-1.

Lü, S., Feng, C., Gao, C., Wang, X., Xu, X., Bai, X., Gao, N. and Liu, M. 2016. Multifunctional environmental smart fertilizer based on l -aspartic acid for sustained nutrient release. *Journal of Agricultural and Food Chemistry* 64(24):4965-4974, doi:10.1021/acs.jafc.6b01133.

Luan, H., Gao, W., Huang, S., Tang, J., Li, M., Zhang, H., Chen, X. and Masiliūnas, D. 2020. Organic amendment increases soil respiration in a greenhouse vegetable production system through decreasing soil organic carbon recalcitrance and increasing carbon-degrading microbial activity. *Journal of Soils and Sediments* 20(7):2877-2892, doi:10.1007/s11368-020-02625-z.

Malik, K., Sharma, A., Harikarthik, D., Rani, V., Arya, N., Malik, A., Rani, S., Sangwan, P. and Bhatia, T. 2023. Deciphering the biochemical and functional characterization of rice straw cultivars for industrial applications. *Heliyon* 9(6):e16339, doi:10.1016/j.heliyon.2023.e16339.

Martiny, T.R., Pacheco, B.S., Pereira, C.M.P., Mansilla, A., Astorga-España, M.S., Dotto, G.L, Moraes, C.C. and Rosa, G.S. 2020. A novel biodegradable film based on κ-carrageenan activated with olive leaves extract. *Food Science and Nutrition* 8(7):3147-3156, doi:10.1002/fsn3.1554.

Masarin, F., Cedeno, F.R.P., Chavez, E.G.S., De Oliveira, L.E., Gelli, V.C. and Monti, R. 2016. Chemical analysis and biorefinery of red algae *Kappaphycus alvarezii* for efficient production of glucose from residue of carrageenan extraction process. *Biotechnology for Biofuels* 9(1):1-12, doi:10.1186/s13068-016-0535-9.

Mohammadi, A., Cowie, A., Mai, T.L.A., De La Rosa, R.A., Brandão, M., Kristiansen, P. and Joseph, S. 2016. Quantifying the greenhouse gas reduction benefits of utilizing straw biochar and enriched biochar. *Energy Procedia* 97:254-261, doi:10.1016/j.egypro.2016.10.069.

Mokolobate, M. and Haynes, R. 2002. Comparative liming effect of four organic residues applied to an acid soil. *Biology and Fertility of Soils* 35:79-85, doi:10.1007/s00374-001-0439-z.

Momesso, L., Crusciol, C.A.C., Bossolani, J.W., Moretti, L.G., Leite, M.F.A., Kowalchuk, G.A. and Kuramae, E.E. 2022. Toward more sustainable tropical agriculture with cover crops: soil microbiome responses to nitrogen management. *Soil and Tillage Research* 224:105507, doi:10.1016/j.still.2022.105507.

Munajad, A., Subroto, C. and Suwarno 2018. Fourier transform infrared (FTIR) spectroscopy analysis of transformer paper in mineral oil-paper composite insulation under accelerated thermal aging. *Energies* 11(2), doi:10.3390/en11020364.

Mutolib, A., Rahmat, A., Triwisesa, E., Hidayat, H., Hariadi, H., Kurniawan, K., Sutiharni, and Sukamto. 2023. Biochar from agricultural waste for soil amendment candidate under different pyrolysis temperatures. *Indonesian Journal of Science and Technology* 8(2):243-258, doi:10.17509/ijost.v8i2.55193.

Nandiyanto, A.B.D., Oktiani, R. and Ragadhita, R. 2019. How to read and interpret FTIR spectroscope of organic material. *Indonesian Journal of Science and Technology* 4(1):97-118, doi:10.17509/ijost.v4i1.15806.

Nardis, B.O., Da Silva Carneiro, J.S., De Souza, I.M.G., De Barros, R.G. and Melo, L.C.A. 2021. Phosphorus recovery using magnesium-enriched biochar and its potential use as fertilizer. *Archives of Agronomy and Soil Science* 67(8):1017-1033, doi:10.1080/03650340.2020.1771699.

Ndoung, O.C.N., de Figueiredo, C.C. and Ramos, M.L.G. 2021. A scoping review on biochar-based fertilizers: enrichment techniques and agro-environmental application. *Heliyon* 7(12), doi:10.1016/j.heliyon.2021.e08473.

Obalum, S.E., Uteau-Puschmann, D. and Peth, S. 2019. Reduced tillage and compost effects on soil aggregate stability of a silt-loam Luvisol using different aggregate stability tests. *Soil and Tillage Research* 189:217-228, doi:10.1016/j.still.2019.02.002.

Petersson, T., Antoniella, G., Chiriacò, M.V., Perugini, L. and Chiti, T. 2024. The misconception of soil organic carbon sequestration notion: When do we achieve climate benefit? *Soil Use and Management* 40(1):1-7, doi:10.1111/sum.13009.

Phuong, D.T.M., Miyanishi, T., Okayama, T. and Kose, R. 2016. Pore characteristics and adsorption capacities of biochars derived from rice residues as affected by variety and pyrolysis temperature. *American Journal of Innovative Research and Applied Sciences* 2(5):179-189.

Pituello, C., Ferro, N.D., Francioso, O., Simonetti, G., Berti, A., Piccoli, I., Pisi, A. and Morari, F. 2018. Effects of biochar on the dynamics of aggregate stability in clay and sandy loam soils. *European Journal of Soil Science* 69(5):827-842, doi:10.1111/ejss.12676.

Purwanto, B.H. and Alam, S. 2020. Impact of intensive agricultural management on carbon and nitrogen dynamics in the humid tropics. *Soil Science and Plant Nutrition* 66(1):50-59, doi:10.1080/00380768.2019.1705182.

Rakian, T.C., Kilowasid, L.M.H., Afa, L.O., Riskyana, A., Nurazizah, Wijayanti, Y., Bahrun, A., Subair, I., Rahni, N.M, Sarawa, A.S. and Karimuna, L. 2023. Soil biological quality in rhizosphere, growth, and yield of upland rice grown on acid soil after amended biochar enriched sap of *Kappaphycus alvarezii*. *Biodiversity* 24(12):6780-6792, doi:10.13057/biodiv/d241241.

Ramírez, P.B., Machado, S., Singh, S., Plunkett, R. and Calderón, F.J. 2023. Addressing the effects of soil organic carbon on water retention in US Pacific Northwest wheat–soil systems. *Frontiers in Soil Science* 3, doi:10.3389/fsoil.2023.1233886.

Shan, Y. and Riaz, A. 2023. The single and interactive effects of aluminium and low pH, or Ca/Al ratios on red pine seedlings. *BMC Research Notes* 16(1):1-7, doi:10.1186/s13104-023-06609-3.

Shi, Y., Yu, Y., Chang, E., Wang, R., Hong, Z., Cui, J., Zhang, F., Jiang, J. and Xu, R. 2023. Effect of biochar incorporation on phosphorus supplementation and availability in soil: a review. *Journal of Soils and Sediments* 23(2):672-686.

Shu, X., Tian, W., Xiong, S., Zhang, W. and Zhang, Q. 2022. Straw biochar at different pyrolysis temperatures passivates pyrite by promoting electron transfer from biochar to pyrite. *Processes* 10(10):1-12, doi:10.3390/pr10102148.

Simatupang, N.F., Pong-Masak, P.R., Ratnawati, P., Agusman, Paul, N.A. and Rimmer, M.A. 2021. Growth and product quality of the seaweed *Kappaphycus alvarezii* from different farming locations in Indonesia.

Aquaculture Reports 20, doi:10.1016/j.aqrep.2021.100685.

Soliman, E. and Mansour, M.M. 2024. Enhancing soil organic carbon content and water retention using polyvinyl alcohol cross-linked with chitosan and pectin. *Journal of Soil Science and Plant Nutrition* 24(1):791-803, doi:10.1007/s42729-023-01584-x.

Song, J., Jin, X., Wang, X.C. and Jin, P. 2019. Preferential binding properties of carboxyl and hydroxyl groups with aluminium salts for humic acid removal. *Chemosphere* 234:478-487, doi:10.1016/j.chemosphere.2019.06.107.

Stocking, M.A. 2003. Tropical soils and food security: the next 50 years. *Science* 302(5649):1356-1359, doi:10.1126/science.1088579.

Sudhakar, M.P., Peter, D.M. and Dharani, G. 2021. Studies on the development and characterization of bioplastic film from the red seaweed (*Kappaphycus alvarezii*). *Environmental Science and Pollution Research* 28(26):33899-33913, doi:10.1007/s11356-020-10010-z.

Um-E-laila, Hussain, A., Nazir, A., Shafiq, M. and Firdaus-E-bareen. 2021. Potential application of biochar composite derived from rice straw and animal bones to improve plant growth. *Sustainability* 13(19), doi:10.3390/su131911104.

van Tol de Castro, T.A., Tavares, O. C. H., de Oliveira Torchia, D. F., Pereira, E.G., Rodrigues, N.F., Santos, L.A.... and García, A.C. 2024. Regulation of growth and stress metabolism in rice plants through foliar and root application of seaweed extract from *Kappaphycus alvarezii* (Rhodophyta). *Journal of Applied Phycology*, doi:10.1007/s10811-024-03216-y.

Wagner, S., Cattle, S. and Scholten, T. 2007. Soil-aggregate formation as influenced by clay content and organic-matter amendment. *Journal of Plant Nutrition and Soil Science* 170:173-180, doi:10.1002/jpln.200521732.

Wang, X., Zhu, Z., Huang, N., Wu, L., Lu, T. and Hu, Z. 2023. Impacts of biochar amendment and straw incorporation on soil heterotrophic respiration and desorption of soil organic carbon. *Geoscience Letters* 10(1), doi:10.1186/s40562-023-00285-8.

Xiao, X., Chen, B. and Zhu, L. 2014. Transformation, morphology, and dissolution of silicon and carbon in rice straw-derived biochars under different pyrolytic temperatures. *Environmental Science and Technology* 48(6):3411-3419, doi:10.1021/es405676h.

Yang, C., Liu, J. and Lu, S. 2021. Pyrolysis temperature affects pore characteristics of rice straw and canola stalk biochars and biochar-amended soils. *Geoderma* 397:115097, doi:10.1016/j.geoderma.2021.115097.

Yang, L., May, P.W., Yin, L., Smith, J.A. and Rosser, K.N. 2007. Ultra fine carbon nitride nanocrystals synthesized by laser ablation in liquid solution. *Journal of Nanoparticle Research* 9(6):1181-1185, doi:10.1007/s11051-006-9192-4.

Yew, Y.P., Shameli, K., Miyake, M., Kuwano, N., Bt Ahmad Khairudin, N.B., Bt Mohamad, S.E. and Lee, K.X. 2016. Green synthesis of magnetite (Fe_3O_4) nanoparticles using seaweed (*Kappaphycus alvarezii*) extract. *Nanoscale Research Letters* 11(1), doi:10.1186/s11671-016-1498-2.

Yuan, J., Shengzhe, E. and Che, Z. 2022. Base cation-enhancing role of corn straw biochar in an acidic soil. *Soil Use and Management* 38(2):1322-1336, doi:10.1111/sum.12782.

Zhang, S., Gong, W., Wan, X., Li, J., Li, Z., Chen, P., Xing, S., Li, Z. and Liu, Y. 2024. Influence of organic matter input and temperature change on soil aggregate-associated respiration and microbial carbon use efficiency in alpine agricultural soils. *Soil Ecology Letters* 6(3), doi:10.1007/s42832-023-0220-4.

Zhang, S., Zhu, Q., Vries, W., Ros, G., Chen, X., Muneer, M., Zhang, F. and Wu, L. 2023. Effects of soil amendments on soil acidity and crop yields in acidic soils: A world-wide meta-analysis. *Journal of Environmental Management* 345, doi:10.1016/j.jenvman.2023.118531.

Zheng, H., Liu, D., Liao, X., Miao, Y., Li, Y., Li, J., Yuan, J., Chen, Z. and Ding, W. 2022. Field-aged biochar enhances soil organic carbon by increasing recalcitrant organic carbon fractions and making microbial communities more conducive to carbon sequestration. *Agriculture, Ecosystems and Environment* 340:108177, doi:10.1016/j.agee.2022.108177.

Zhou, G., Zhou, X., Zhang, T., Du, Z., He, Y., Wang, X., Shao, J., Cao, Y., Xue, S., Wang, H. and Xu, C. 2017. Biochar increased soil respiration in temperate forests but had no effects in subtropical forests. *Forest Ecology and Management* 405:339-349, doi:10.1016/j.foreco.2017.09.038.